Malaysian Journal of Analytical Sciences (MJAS)
Published by Malaysian Analytical Sciences Society

POLYMER-FREE TRANSFER OF GRAPHENE-BASED MATERIAL DERIVED FROM COOKING PALM OIL BY CHEMICAL VAPOUR DEPOSITION TECHNIQUE

(Pemindahan Bebas Polimer bagi Bahan Berasaskan Grafin yang Disintesis dari Minyak Masak Kelapa Sawit Menggunakan Teknik Pemendapan Wap Kimia)

Azzafeerah Mahyuddin[1,2*], Abd. Khamim Ismail[1], Muhammad Firdaus Omar[1], Ainul Hakimah Karim[3]

[1]Department of Physics,
Faculty of Science, Universiti Teknologi Malaysia, 81310 Johor, Malaysia
[2]Department of Quality Engineering,
Universiti Kuala Lumpur, Malaysian Institute of Industrial Technology,
Persiaran Sinaran Ilmu, Bandar Seri Alam, 81750 Johor, Malaysia.
[3]Department of Instrumentation and Control Engineering,
Universiti Kuala Lumpur, Malaysian Institute of Industrial Technology,
Persiaran Sinaran Ilmu, Bandar Seri Alam, 81750 Johor, Malaysia.

[*]Corresponding author: azzafeerah@unikl.edu.my

Received: 17 December 2021; Accepted: 10 March 2022; Published: 30 October 2022

Abstract

Chemical vapour deposition (CVD) of cooking palm oil precursors with a nickel (Ni) catalyst is an established method to produce graphene-based materials. Nonetheless, transferring the graphene sheets from the substrate surface to a selected target substrate presents a major challenge. The utilisation of well-known poly (methyl methacrylate) (PMMA)-assisted graphene transfer promotes defects, impurities, folds, and wrinkles in the graphene sheets, thus affecting its properties. Consequently, the present study demonstrated a polymer-free graphene sheets transfer technique on a Ni substrate derived from cooking palm oil. A dropwise hexane layer substituted the PMMA supporting layer during the etching process to remove the Ni substrate. The quality of the graphene sheet was investigated with optical microscopy by employing a Leica DM1750 M microscope, scanning electron microscopy (SEM) with a Hitachi S-3400N, and Raman spectroscopy utilising a UniDRON automated microscope Raman mapping system with 514 nm laser excitation. Resultantly, macroscopically clean and crack-free graphene sheets were was obtained. Furthermore, the technique was less complicated than the PMMA-assisted transfer technique. The Raman spectra of the polymer-free method also revealed visible graphene peaks, which was absent in the PMMA-transferred samples.

Keywords: graphene, chemical vapour deposition, polymer-free transfer

Abstrak

Kaedah pemendapan wap kimia (CVD) yang menggunakan minyak masak kelapa sawit sebagai prekursor serta nikel sebagai pemangkin dalam proses sintesis bahan berasaskan grafin merupakan teknik yang telah lama dikenali. Namun, cabaran utama dalam menggunakan teknik CVD ini ialah proses pemindahan helaian grafin dari permukaan substrat asal ke substrat baru. Salah

satu kaedah pemindahan yang sering digunakan ialah kaedah pemindahan poli (metil-metakrilat) (PMMA) iaitu sejenis polimer yang akan menyebabkan helaian grafin mengalami kerosakan seperti kotor, berlipat dan berkedut. Oleh yang demikian, kajian ini akan menampilkan suatu teknik pemindahan grafin yang bebas polimer, disintesis di atas substrat nikel menggunakan minyak masak kelapa sawit. Lapisan heksana digunakan sebagai pengganti lapisan PMMA semasa proses penghakisan substrat nikel. Kualiti helaian grafin daripada hasil proses pemindahan ini dikaji menggunakan mikroskop optik (Leica DM1750 M), mikroskop pengimbasan elektron (SEM) dari Hitachi S-3400N dan spektroskopi Raman (system pemetaan mikroskop automatik Raman UniDRON dengan pengujaan laser 514 nm). Dapatan menunjukkan bahawa kaedah ini dapat menghasilkan helaian grafin yang bersih, tidak koyak serta pemprosesan yang tidak rumit berbanding teknik PMMA. Kaedah bebas polimer ini juga dapat menerbitkan puncak grafen menggunakan spektroskopi Raman berbanding kaedah pemindahan PMMA.

Kata kunci: grafin, kaedah pemendapan wap kimia, pemindahan bebas polimer

Introduction

Graphene is a two-dimensional (2D) substance comprising sp^2 carbon atoms in a gigantic aromatic structure [1]. The extraordinary performance of graphene in electrical [2], mechanical [3], and chemical [4] applications are promising, but previous studies revealed several gaps and shortcomings of the material. For instance, high-quality large-area graphene is not defect-free. Generally, graphene is synthesised through various methods, including mechanical, liquid, and chemical exfoliations, thermal decomposition of silicon carbide, chemical synthesis, and chemical vapour deposition (CVD). Among the techniques, CVD has been investigated as an alternative method to overcome inherent limitations in manufacturing large-area graphene with uniform thickness, high crystallinity, and fewer defects [5,6]. Traditional CVD techniques employ purified gaseous precursors, which are expensive, explosive, and require high-temperature growth, and accordingly, carbon waste has become a substitute precursor to synthesising functional carbonaceous material, such as graphene. The capability to fabricate graphene from such economic precursors would be cost-effective and sustainable for practical applications [7].

Recent studies have investigated the utilisation of several renewable natural carbon precursor sources for graphene production, namely camphor [8], reed (grass family) [9], cookies, chocolate, grass, roaches, dog faeces [10], and rice husks [11]. Numerous research reported employing cooking oil to manufacture graphene [12–14]. Most graphene growth via the CVD technique implement a post-grow polymer transfer from the surface catalyst onto the target substrate. The method introduces a complicated process in which a thin polymer layer is deposited on a graphene sheet that acts as a support to remove the metallic substrate by wet etching. The procedure induces defects, wrinkles, impurities, cracks, and stubborn polymer residues [15], which might obstruct the performance of graphene in subsequent applications [16, 17]. The graphene must be free to appreciate its extraordinary properties fully. Consequently, alternative routes of transfer methods such as polymer-free techniques are being explored to resolve the contamination problems [18, 19].

The main objective of the current work was to investigate a polymer-free method for improving the graphene transfer process synthesised from cooking palm oil through the CVD technique. The polymer-free approach employed hexane as a low-viscosity liquid organic layer, which would be very beneficial to stabilise and safeguard the graphene-based sheet generated during the metal substrate wet etching. The present study utilised hexane as the organic layer as it lacks heteroatoms and aromatic groups and is very volatile. Essentially, hexane could serve as a more efficient alternative to the polymer layer deposited on the graphene sheets in most currently practised transfer methods. A comparison study with the poly (methyl methacrylate) (PMMA) transfer method was also performed.

Materials and Methods

The CVD graphene growth

The graphene-based films in the present study were synthesised in a conventional CVD system equipped with a vacuum and argon (Ar) gas purging system. First, nickel (Ni) sheets were cut into 1 cm × 1 cm pieces and subjected to a specific cleaning protocol. Subsequently,

the Ni pieces were loaded into a CVD chamber to eliminate organic contaminations, impurities, and oil to increase the adhesion of the fabricated films on the substrate. The cleaning process began with an ultrasonic bath in ethanol for 10 minutes, followed by rinsing with distilled water. The metal sheets were then cleaned in isopropyl alcohol (IPA) for ten minutes, washed with distilled water, and blown dry with nitrogen (N_2) gas.

Graphene growth was conducted in a conventional thermal CVD furnace with a quartz tube. Two alumina boats were positioned in the heating region of the tube furnace. One boat was filled with a millilitre of cooking palm oil precursor, while the other contained several pieces of Ni sheets. The boat filled with the cooking palm oil precursor was covered with aluminium foil with tiny holes to avoid oil spillage during the heating process. The ends of the quartz tube were sealed. The air and impurities in the tubes were evacuated with a vacuum pump prior to purging with Argon (Ar) gas. The evacuation and Ar purging processes took approximately 30 minutes.

At this point, both boats filled with cooking palm oil and Ni sheets were present during the evacuation process. Subsequently, while the reaction tubes were in the Ar environment, the furnace temperature was raised to 400 ℃ at a 30 ℃ min^{-1} rate. The temperature was maintained for five minutes, during which the cooking palm oil was expected to reach its vaporisation point and flow towards the Ni sheets to start the graphene-based material growth. Subsequently, the furnace was switched off, and the sample was cooled to room temperature. After the effective thermal decomposition mechanism, carbon (C) from the vapourised cooking palm oil was anticipated to disperse evenly on the heated substrate surface.

Polymer-free graphene transfer

Sandpaper mechanical polishing was utilised to eliminate graphene-based material films on the backside of the Ni sheet. The sample was then subjected to metal etching. The graphene-based/Ni was gently placed onto the surface of 0.1 M iron (III) chloride [($FeCl_3$), System ≥ 98%] aqueous solution. Subsequently, the sample was floated (graphene-based side up) atop $FeCl_3$ solution (10 mL) for approximately a few seconds before a layer of hexane (Merck, ≤ 100%) was gently added to the top with a dropper. The hexane layer ensured that the graphene was not torn due to the surface tension associated with the etchant solution.

The Ni etching occurred in the $FeCl_3$ solution for approximately five hours, with the graphene-based sheet layer remaining trapped at the hexane and $FeCl_3$ aqueous solution interface. After etching, only the graphene sheet remained floating between the hexane and $FeCl_3$ solution, whereas the Ni sheet had fully submerged to the bottom of the etchant solution. The graphene sheet was then scooped out with a clean glass slide that was cleaned in a hot acetone bath for 10 minutes, methanol for 5 minutes, and rinsed with distilled water.

The sheet was transferred to a hexane/water interface at one to one ratio. The step was conducted to remove any remaining salt particles and debris from the back of the graphene layer. The graphene sheet was removed with a glass slide and let dry at room temperature after several hours. Fundamentally, the lack of heteroatoms and aromatic groups and volatility and rapid evaporation of hexane enabled the vapourisation and removal of hexane residues at room temperature.

The standard poly (methylmethacrylate) (PMMA) transfer method was performed on a sample set for comparison purposes. According to previous works, the polymer films were designed to protect graphene, which is fragile and could break. The solid support also helps reduce graphene wrinkles from the thermal expansion coefficient between the metal substrate and graphene.

A PMMA layer was spin-coated onto the surface of the graphene/Ni sheet at 1200 rpm for 30 s. Subsequently, the layer was annealed at 80℃ for 15 min to cure it, followed by etching in $FeCl_3$ to eliminate the Ni sheet. After an appropriate etching time, a clean glass slide was employed to scoop out the PMMA/graphene sheet. The sheet was rinsed with distilled water and baked at 60℃ for five minutes. The step was necessary to enhance contact adhesion and eliminate trapped water.

The second layer of PMMA was spin-coated on top of

the PMMA/graphene sheet and let dry at room temperature. Subsequently, the PMMA layer was washed with acetone and rinsed with distilled water. Finally, the graphene sheet was transferred to a clean glass substrate. The second PMMA layer was developed to reduce cracks in the transferred graphene [20]. Without the second layer of PMMA, tension might be imposed, resulting in large cracks on the graphene after the transfer process.

Sample characterisation

Evaluation of the initial quality of the graphene-based sheet was performed through optical microscopy by employing a material analysis microscope Leica DM1750 M. The surface morphology was assessed utilising scanning electron microscopy (SEM) (Hitachi S-3400N). Raman spectroscopy was conducted with UniDRON Automated Microscope Raman mapping system equipped with 514 nm laser excitation.

Results and Discussion

Optical microscopy

Optical microscopy analysed the coverage and distribution of the graphene-based films prior- and post-transfer process. Figure 1 displays the optical images of the graphene-based films on the Ni sheets after the CVD furnace growth process. Yellow, brown, purple, and grey layers covered the Ni sheet entirely. Similar results were reported by [12] as the colour might be the initial information of the graphene-based film structure.

The samples were subjected to two graphene transfer processes following the growth process, the PMMA and polymer-free transfers. Figure 2 illustrates the optical microscopy images of the graphene-based films after being polymer-free transferred on the glass substrate. A complete graphene-based film was obtained after transfer. The films exhibited colourful patterns dominated by grey and yellow. Some brownish colour from $FeCl_3$ residue was observed in the optical images, which was reported commonly occurring in transfer-free methods [21]. The phenomenon might arise from the graphene/Ni sample not correctly floated on the etching solution and correctly trapped in the hexane/ $FeCl_3$ solution interface. Moreover, the "soft support" from the hexane solution might be contaminated with the $FeCl_3$ etching solution.

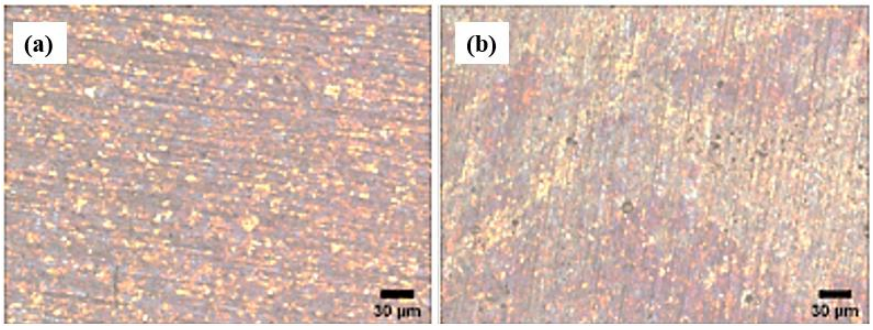

Figure 1. The optical images of two sample pieces of the graphene-based structure on Ni sheet grown at 400 °C

Due to cracks, the graphene-based films transferred with the PMMA technique demonstrated poor film quality. Additionally, some parts of the films were folded during the transfer process. The PMMA transfer process is often intricate, and the free-standing graphene could be broken due to surface tension as it dries [21]. Furthermore, some films failed to attach to the glass substrates, tended to break away, and immediately produced cracks when acetone dissolved the PMMA layer.

Trapped water between the PMMA and graphene and glass substrate throughout the transfer procedure might lead to folded layers and wrinkles. Consequently, the polymer-free transfer method offered a better option for transferring graphene-based films onto the desired substrate. Nonetheless, improvements to minimise the residues might be necessary for future works.

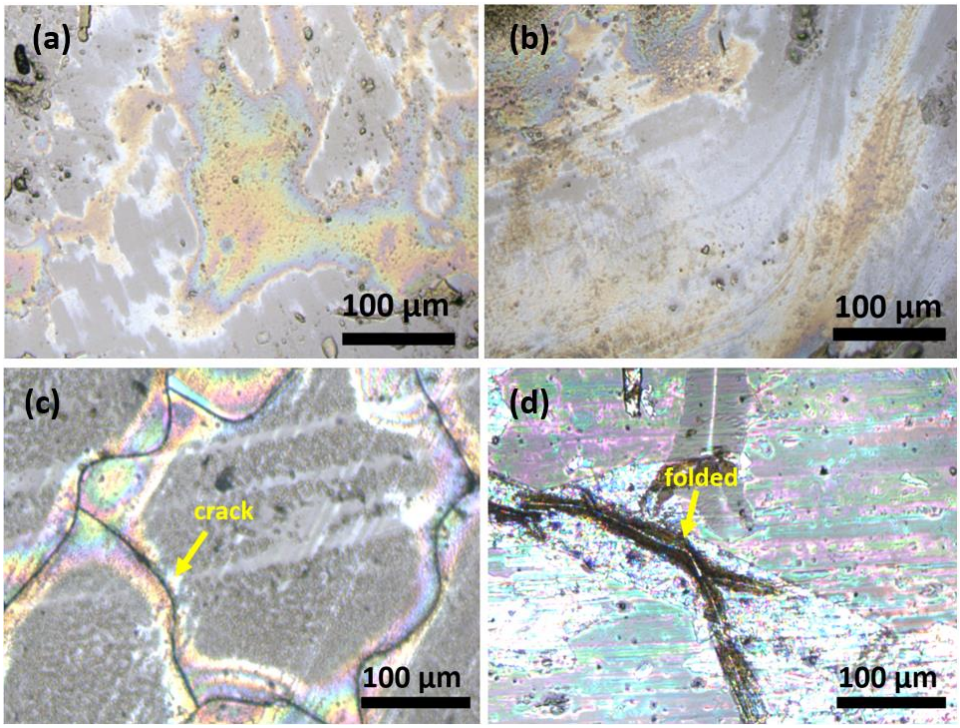

Figure 2. The optical images of the polymer transfer-free samples, denoted (a) and (b), and the PMMA transfer samples, represented by (c) and (d)

Scanning electron microscopy

The graphene films transfer is a crucial process that could affect the quality and performance of graphene in devices. Consequently, SEM was employed to record the surface morphology of the graphene films post-transfer onto the glass substrate. The measurements would further confirm the optical analysis results. Figure 3 exhibits the two specific spots focused on for the SEM assessment.

The PMMA transferred film sample observed suffered folded films and was heavily contaminated with PMMA residue. Although acetone wash was performed several times during the transfer process, the films still contained the residue. Meanwhile, the polymer-free transfer sample demonstrated a much cleaner and smoother surface. The low viscosity of the hexane layer on top of an aqueous etchant layer stabilised and safeguarded the free-standing graphene layer created during the Ni wet etch and water rinse.

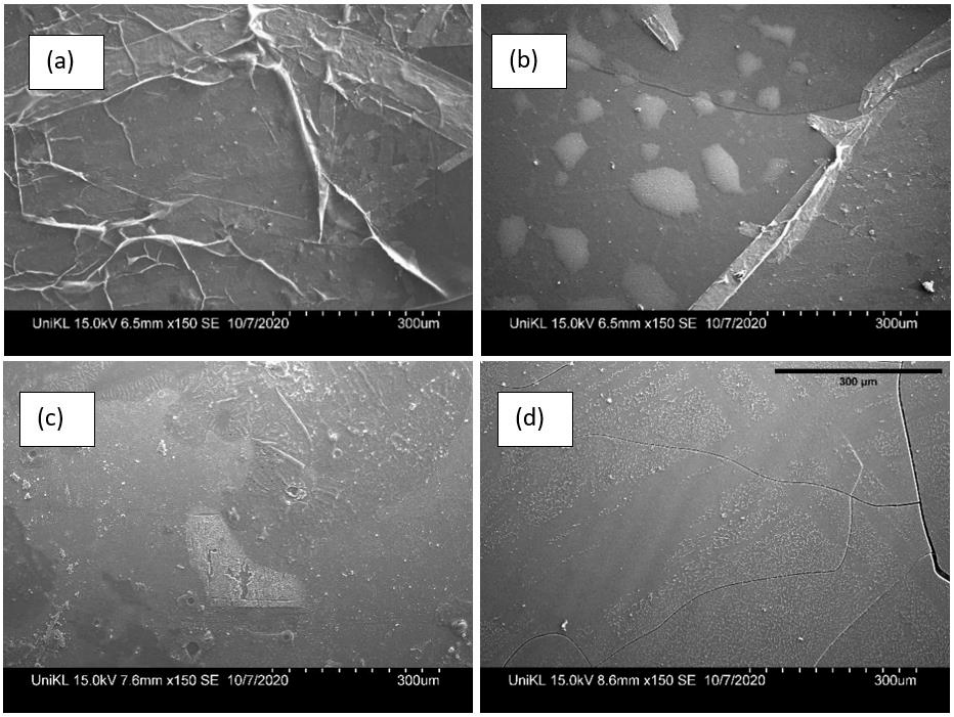

Figure 3. The SEM images of the graphene-based materials (a) and (b) after PMMA and (c) and (d) polymer-free transferred

Fundamentally, the hexane layer substituted the polymer layers currently employed in most graphene transfer procedures. The hexane layer prevented the graphene films from breaking due to the surface tension of the etching solution. The lack of heteroatoms and aromatic groups and high volatility of hexane resulted in no debris left on the graphene surface when transferred to the preferred substrate [19].

Raman spectroscopy

Raman analyses were performed on both samples to examine the synthesised graphene-based films. Figure 4 displays the Raman spectra of the films after being transferred onto the glass substrate utilising two different methods. No graphene structure was formed on the PMMA transfer samples and only PMMA peaks were detected (represented by pink dots). The observation might be due to the PMMA films not being fully dissolved with acetone. The films transferred with the polymer-free method exhibited two peaks that correlated to the D and G bands. The D band was observed at ~1348 cm^{-1}, while the G band was located at ~1543 cm^{-1}. For the sample analysed, the D and G bands demonstrated broad peaks, with no 2D peak, implying that the sample was a graphene oxide (GO) film. A previous study reported similar GO Raman spectra [22].

The D band peak was attributed to the structural defects and disorder of the graphite surfaces [23]. The G band was associated with the radial C-C stretching of the sp^2 bonded carbon [23]. Furthermore, the intensity of the D band peak to the intensity of the G band peak (I_D/I_G) ratio provided details on the defect density of the graphic structure. The I_D/I_G ratio for the GO sample was 0.99. The ratio would be helpful in future studies on the growth kinetics of the films. Shah et al. stated that as the rate of I_D/I_G decreased, the defects in the films were reduced, resulting from nucleation and the joining of the individual nucleation islands [24].

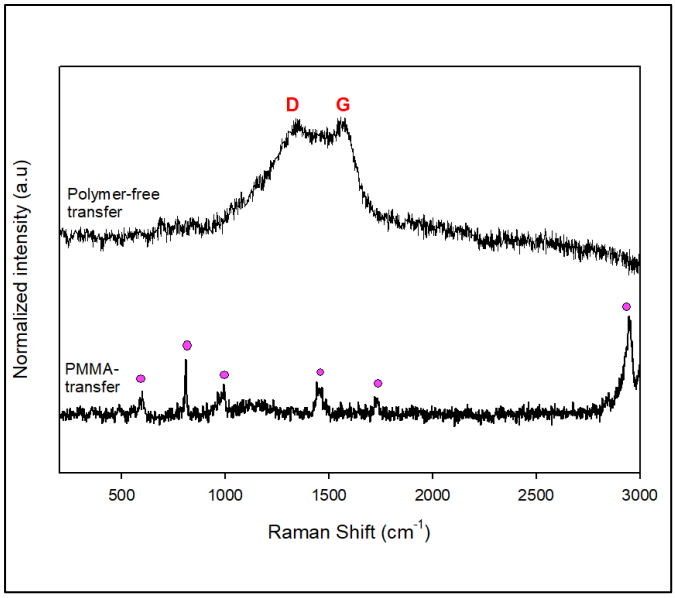

Figure 4. The Raman spectra of the PMMA transferred (bottom) and (above) polymer-free transferred samples

The multiple Raman spectra of four spots on the polymer-free transferred samples are displayed in Figure 5. Two peaks were detected at ~1354 cm^{-1} and ~1540 $cm^{-1,}$ respectively, thus corresponding to D and G peaks. No 2D peak (theoretically at 2670 cm^{-1}) was detected at any spot. Incomplete graphene film formation was observed at spots 1 and 2, which might be due to the lack of energy required for graphene formation to detach and transform the precursor material (hydrocarbon species).

Notably, the low growth temperature of 400°C was insufficient to decompose carbon feedstock from cooking palm oil. Nevertheless, the results might be fundamental in designing a CVD experimental setup. A similar situation was observed in soybean oils-graphene [25]. In the initial stages of the annealing process, the long carbon chains in the soybean oil precursor were thermally detached into methyl and ethyl gaseous carbon atoms. As the growth temperature was increased to 800°C, the carbon-building units began detaching into carbon atoms and dissolve into the Ni bulk. The short duration of the annealing process would then promote carbon atom dissolution in the Ni substrate. In particular, excessive precursor material preceded an oversaturation of deposited carbon in the bulk of the Ni and crystallised the graphite on the Ni surfaces.

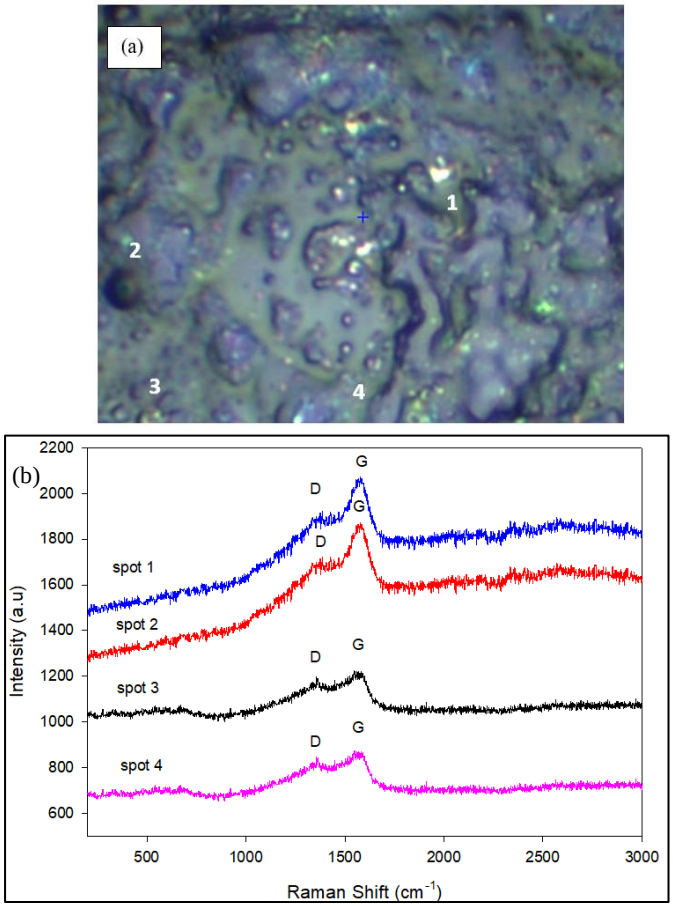

Figure 5. The (a) Four Raman mapping spots and (b) multiple Raman spectrum of the graphene films on a glass substrate of the polymer-free transferred sample

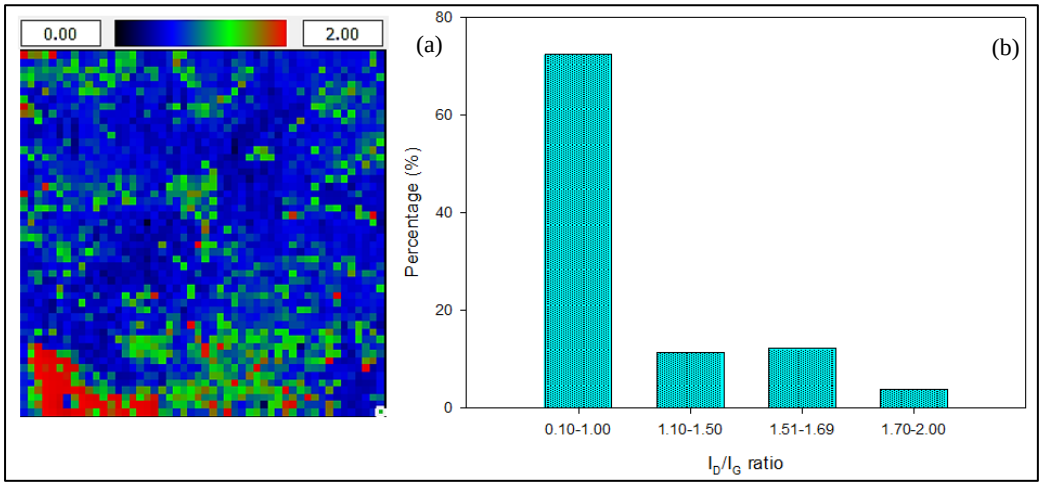

Figure 6. The (a) Raman mapping image of the graphene films on a glass substrate with I_D/I_G ratio within a 2 µm × 2 µm area and (b) histograms of the I_D/I_G ratio intensity percentages

Based on the Raman mapping of the I_D/I_G ratio and the intensity of the GO sample in Figure 6, the grown film was not uniformly distributed on the substrate. The non-uniform colour distribution provided fundamental knowledge of the substrate. The current study employed Ni polycrystalline sheet that was not subjected to polishing and etching treatment. The Ni surfaces in the carbon/polycrystalline Ni combination was densely populated by grain boundaries, particularly interplane grain boundaries, allowing carbon to accumulate throughout the segregation phase. Meanwhile, the single-crystalline surface on Ni (111) was very smooth, with almost no grain boundaries, allowing uniform carbon segregation, forming single-layer graphenes [26].

Histograms derived from the Raman mapping indicated the I_D/I_G ratio percentages. The ratio was divided into four groups, which corresponded to the most prominent family colours in the Raman mapping image, such as blue, dark green, light green, and red. Resultantly, the blue pixels were accounted for a ratio of less than 1.00, while the light green pixels had a 1.10–1.50 ratio, the dark green pixels exhibited a 1.51–1.69 ratio, and the red pixels was at a 1.70–2.00 ratio.

The counted pixels were presented in a histogram as a function of percentage. From the histogram, 70% of the I_D/I_G ratio was denominated by a ratio of less than 1.00. Meanwhile, 12, 11, and 3% corresponded to 1.51–1.69, 1.10–1.50, and 1.70–2.00 ratios, respectively. A high I_D/I_G ratio value corresponded to the high value of defects and disorders in the films [27]. Since 70% of the sample exhibited a ratio of less than 1.00, the film probably has a low value of defect and disorder. Consequently, hexane-assisted transfer promoted a clean graphene layer which might have enhanced the fundamental studies of graphene transfer.

Conclusion

The current study has successfully demonstrated an efficient polymer-free method to transfer graphene-based material sheets onto a substrate. The method was polymer contamination- and wrinkle-free. Compared to the PMMA transfer technique, the polymer-free method was easier to implement and less complicated. A significant advantage of hexane, contradictory to PMMA, was a smaller molecule with its high volatility, simplifying elimination from the graphene. The Raman studies demonstrated fundamental information in developing high-quality graphene-based material for future applications.

Acknowledgement

The authors would like to extend their gratitude to the Ministry of Higher Education for supporting the study under the FRGS, Registration Proposal No: FRGS/1/2019/STG07/UTM/02/17 (Vot no: R.J130000.7854.5F236). The work was also funded by the short-term research grant (str19062) from Universiti Kuala Lumpur-Malaysian Institute of Industrial Technology (UNIKL MITEC).

References

1. Novoselov, K. S., Geim, A. K., Morozov, S. V., Jiang, D. E., Zhang, Y., Dubonos, S. V., ... and Firsov, A. A. (2004). Electric field effect in atomically thin carbon films. *Science,* 306(5696): 666-669.
2. Avouris, P. (2010). Graphene: Electronic and photonic properties and devices. *Nano Letters*, 10(11): 4285-4294
3. Lee, C., Wei, X., Kysar, J.W., and Hone, J. (2008). Measurement of the elastic properties and intrinsic strength of monolayer graphene. *Science*, 321(5887): 385-388.
4. Paulus, G. L. C., Wang, Q. H. and Strano, M. S. (2013). Covalent electron transfer chemistry of graphene with diazonium salts. *Accounts of Chemical Research*, 46(1): 160-170.
5. Muñoz, R. and Gómez-Aleixandre, C. (2013). Review of CVD synthesis of graphene. *Chemical Vapor Deposition*, 19: 297-322
6. Yan, Z., Peng, Z. and Tour, J. M. (2014). Chemical vapor deposition of graphene single crystals. *Accounts of Chemical Research*, 47(4): 1327-1337
7. Kwon, S.-J., Seo, H.-K., Ahn, S. and Lee, T.-W. (2019). Value-added recycling of inexpensive carbon sources to graphene and carbon nanotubes. *Advanced Sustainable Systems*, 3(1): 1800016.

8. Aryal, H. R., Adhikari, S., Uchida, H., Wakita, K. and Umeno, M. (2016). Few layers isolated graphene domains grown on copper foils by microwave surface wave plasma CVD using camphor as a precursor. *2D Materials*, 3(1): 011009.
9. Rahbar Shamskar, K., Rashidi, A., Aberoomand Azar, P., Yousefi, M. and Baniyaghoob, S. (2019). Synthesis of graphene by in situ catalytic chemical vapor deposition of reed as a carbon source for VOC adsorption. *Environmental Science and Pollution Research*, 26(4): 3643-3650.
10. Ruan, G., Sun, Z., Peng, Z., and Tour, J. M. (2011). Growth of graphene from food, insects, and waste. *ACS Nano*, 5 (9): 7601-7607
11. Wang, Z., Yu, J., Zhang, X., Li, N., Liu, B., Li, Y., ... and Sun, L. (2016). Large-scale and controllable synthesis of graphene quantum dots from rice husk biomass: a comprehensive utilization strategy. *ACS Applied Materials & Interfaces*, 8(2): 1434-1439.
12. Rahman, S. F. A., Mahmood, M. R. and Hashim, A. M. (2014). Growth of graphene on nickel using a natural carbon source by thermal chemical vapor deposition. *Sains Malaysiana*, 43(8): 1205-1211.
13. Salifairus, M. J., Abd Hamid, S. B., Soga, T., Alrokayan, S. A., Khan, H. A. and Rusop, M. (2016). Structural and optical properties of graphene from green carbon source via thermal chemical vapor deposition. *Journal of Materials Research*, 31(13): 1947-1956.
14. Maarof, S., Ali, A. A. and Hashim, A. M. (2019). Synthesis of large-area single-layer graphene using refined cooking palm oil on copper substrate by spray injector-assisted CVD. *Nanoscale Research Letters*, 14(1): 143.
15. Chen, Y., Gong, X. and Gai, J. (2016). Progress and challenges in transfer of large-area graphene films. *Advanced Science*, 3(8): 1500343
16. Ng, J., Jones, T., Martinez-Velis, I., Wang, A., Hopkins, J. and Xie, Y. H. (2020). Effects of polymer residue on the pull-in of suspended graphene. *Journal of Vacuum Science & Technology B, Nanotechnology and Microelectronics: Materials, Processing, Measurement, and Phenomena*, 38(2): 023001.
17. Stehle, Y. Y., Voylov, D., Vlassiouk, I. V., Lassiter, M. G., Park, J., Sharma, J. K. ... and Polizos, G. (2017). Effect of polymer residues on the electrical properties of large-area graphene–hexagonal boron nitride planar heterostructures. *Nanotechnology*, 28(28): 285601.
18. Belyaeva, L. A., Fu, W., Arjmandi-Tash, H. and Schneider, G. F. (2016). Molecular caging of graphene with cyclohexane: transfer and electrical transport. *ACS Central Science*, 2 (12): 904-909.
19. Zhang, G., Güell, A. G., Kirkman, P. M., Lazenby, R. A., Miller, T. S. and Unwin, P. R. (2016). Versatile polymer-free graphene transfer method and applications. *ACS Applied Materials & Interfaces*, 8(12): 8008-8016.
20. Li, X., Zhu, Y., Cai, W., Borysiak, M., Han, B., Chen, D., ... and Ruoff, R. S. (2009). Transfer of large-area graphene films for high-performance transparent conductive electrodes. *Nano Letters*, 9(12): 4359-4363.
21. Suk, J. W., Kitt, A., Magnuson, C. W., Hao, Y., Ahmed, S., An, J., ... and Ruoff, R. S. (2011). Transfer of CVD-grown monolayer graphene onto arbitrary substrates. *ACS Nano*, *5*(9): 6916-6924.
22. Marcano, D. C., Kosynkin, D. V., Berlin, J. M., Sinitskii, A., Sun, Z., Slesarev, A., ... and Tour, J. M. (2010). Improved synthesis of graphene oxide. *ACS Nano*, 4(8): 4806-4814.
23. Kudin, K. N., Ozbas, B., Schniepp, H. C., Prud'Homme, R. K., Aksay, I. A. and Car, R. (2008). Raman spectra of graphite oxide and functionalized graphene sheets. *Nano Letters,* 8(1): 36-41.
24. Shah, J., Lopez-Mercado, J., Carreon, M. G., Lopez-Miranda, A. and Carreon, M. L. (2018). Plasma synthesis of graphene from mango peel. *ACS Omega,* 3(1): 455-463.
25. Seo, D. H., Pineda, S., Fang, J., Gozukara, Y., Yick, S., Bendavid, A., ... and Ostrikov, K. K. (2017). Single-step ambient-air synthesis of graphene from renewable precursors as electrochemical genosensor. *Nature Communications,* 8(1): 1-9.
26. Zhang, Y., Gomez, L., Ishikawa, F. N., Madaria, A., Ryu, K., Wang, C., ... and Zhou, C. (2010). Comparison of graphene growth on single-crystalline and polycrystalline Ni by chemical vapor deposition. *The Journal of Physical Chemistry Letters*, 1(20): 3101-3107.

27. Khalid, A., Mohamed, M. A., and Umar, A. A. (2017). Graphene growth at low temperatures using RF-plasma enhanced chemical vapour deposition. *Sains Malaysiana*, 46 (7): 1111-1117.